

# Damage Effects of Fluid-filled Submunitions by High Velocity Projectile Impact

Zan Yang\*, Zheng Yuan-feng, Yu Qing-bo, and Wang Hai-fu

State Key Laboratory of Explosion Science and Technology, Beijing Institute of Technology, Beijing - 100 081, China

\*E-mail: prai\_z@bit.edu.cn

## ABSTRACT

A series of tests investigating the damage effects of fluid-filled submunitions by high velocity projectile impact were conducted. An analytical model is presented, in which the yaw angle of the projectile was taken into account. Based on the analytical model, the influence of the strike angle, hit-point offset distance and projectile length to diameter ratio on submunition damage ratio were predicted. The analytical results showed a good agreement with the experiments. The submunition damage ratio strongly depends on the hit-point offset distance, showing a significant decrease with increasing hit-point offset distance. For large hit-point offset distance, increasing the length to diameter ratio of the projectile will effectively improve the submunition damage ratio. There is an appropriate yaw angle of the projectile in which the submunition damage ratio will be maximal.

**Keywords:** Hit-to-kill; Simplified payload; Explosively formed projectile; Yaw angle

## 1. INTRODUCTION

Direct hit has become the main kill mode of most missiles today, high relative impact velocity is the impact kinetic energy source for kill vehicle against ballistic missile<sup>1,2</sup>. The key problem is whether the direct hit can effectively destroy the payloads, especially biological/chemical submunition payloads<sup>3-5</sup>. Direct hit missiles are currently recognised as the only accepted way of killing all payloads of chemical submunitions<sup>6</sup>.

Over the last 20 year, many studies have been carried out experimentally and theoretically on the damage effect of targets by high velocity projectile impact<sup>7-13</sup>. Børvik and colleagues examined the ballistic penetration of steel plates by cylindrical projectiles by experimental, analytical, and numerical investigations<sup>14</sup>. American Lockheed Martin Corporation's McHenry established ALPHA-KV and OPTKV analysis model all based on Tate's penetration theory<sup>15</sup>. The volume overlap analysis model was proposed by Doup<sup>16</sup>. The shot line technology was applied to evaluate the killed fraction of submunition<sup>17</sup>. The US Los Alamos National Laboratory has developed a smooth particle hydrocode SPHINX that is widely used to compute direct hit damage<sup>18</sup>.

For normal impact, the deepest penetration is achieved when the projectile moves along its axis. Oblique and yawed impact will significantly decrease the penetration depth. The yaw angle and oblique angle will affect the overall damage effect, which can be validated by experimental data<sup>19-21</sup>.

However, the mechanical behaviour of high velocity collision between the projectile and the ballistic missile payload would be extremely complex<sup>22</sup>, and the ground tests

and numerical simulation would be time-consuming<sup>23</sup>, the damage effects of the yaw angle are not well researched by experiment and model combined. Here impact experiments were conducted by using the explosively formed projectiles to understand the damage effects of fluid-filled submunitions by high velocity projectile impact. With an analytical damage model considering the yaw angle, the influences of the strike angle, hit-point offset distance and projectile length to diameter ratio on submunition damage ratio were predicted. The results would provide a useful guide to the improvement of direct hit missiles and damage assessment.

## 2. EXPERIMENTS

### 2.1 Experimental Setup

The simulation submunition payload is as shown in Fig. 1, which included a skin, separators and submunitions. The skin had no top/bottom plates. The materials of the skin and separators were ASTM 1045 steel and 2024 aluminum, respectively (ASTM: American Society for Testing Materials). Sealed water-filled cans were used to simulate the fluid-filled submunitions. The size of cylindrical cans was  $\Phi 53 \times 133$  mm, and the can material was tinplate with a thickness of 0.2 mm<sup>24</sup>. A total of 38 submunitions were arrayed in three layers. The top layer contained a circular array of 8 submunitions while the last two layers contained 12 and 18 submunitions respectively. The submunitions were placed directly on aluminum plate separators. Submunition payload dimension parameters are as listed in Table 1.

Due to the very high relative impact velocity between projectile and target, the large mass of the projectile and the limited experimental conditions, explosively formed projectile (EFP) technology was used in the experiment to obtain a large mass projectile within a velocity range of 2000 m/s to 2500

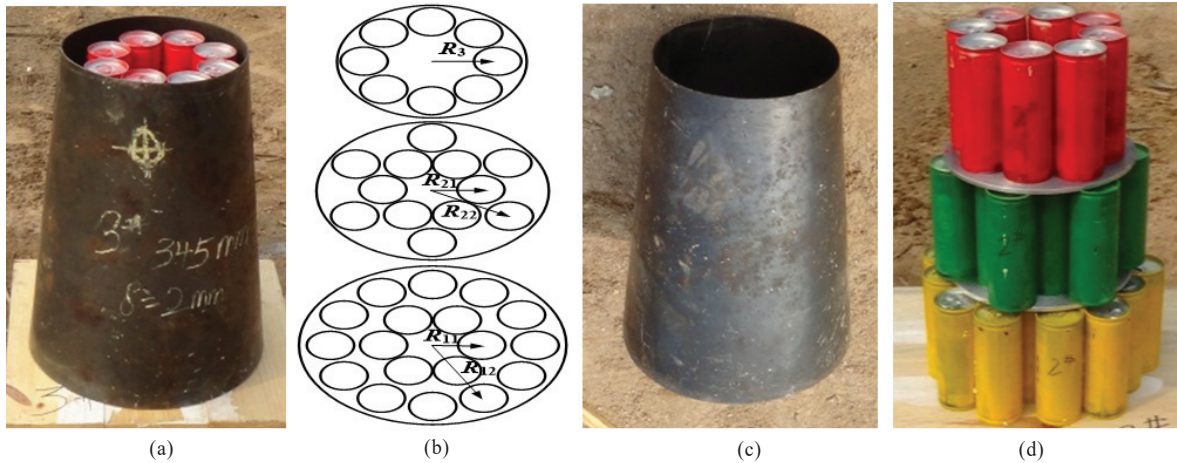


Figure 1. Images of simulated fluid-filled submunition payload: (a) Submunition payload, (b) Submunition arrangement, (c) Payload skin, and (d) Submunitions.

Table 1. Submunition payload dimension parameters

		Shell		Separator		Submunition			
Thickness (mm)	Height (mm)	Top diameter (mm)	Bottom diameter (mm)	Thickness (mm)	R <sub>11</sub> (mm)	R <sub>12</sub> (mm)	R <sub>21</sub> (mm)	R <sub>22</sub> (mm)	R <sub>3</sub> (mm)
2	419	220	320	5	55	115	55	95	75

m/s<sup>25-27</sup>. The experimental device for forming a high velocity projectile is as shown in Fig. 2, which consisted of three parts: the liner, the shell, and the high explosive charge. The cylindrical composition B with a charge diameter (CD) of 90 mm and a length of 180 mm was centrally initiated through a simple detonator. The thickness and mass of the aluminum liner were 13.5 mm (0.15CD) and 252 g, respectively. The thickness of the steel (1006 steel) casing was 7.5 mm. The stand-off-distance between EFP and hit point was 4.0 m. The test principle is as shown in Fig. 3.

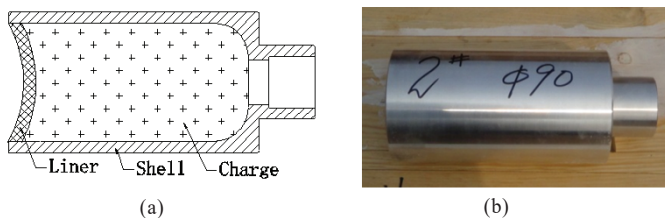


Figure 2. Experimental device forms high velocity projectile: (a) Configuration schematic and (b) Prototype photograph.

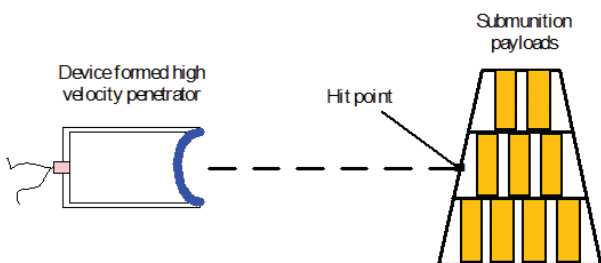


Figure 3. Schematic diagram of test.

## 2.2 Experimental Results

The damage effect of fluid-filled submunitions by high velocity projectile impact is mainly influenced by hit-point offset, impact velocity and yaw. The hit-point offset distance refers to the distance between hit-point and aim point. In the experiment, five typical positions were selected as hit-point. They were the center of the third layer submunitions, the interface between the second layer and the third layer submunitions, the center of the second layer submunitions, the interface between the first layer and the second layer submunitions, and the center of the first layer submunitions. Five dimensionless parameters of hit-point distance are  $\xi = x_a/L_T = -0.34, -0.17, 0, 0.17$  and  $0.34$  respectively,  $x_a$  is axis position from geometric center of payload to hit-point (positive toward bottom),  $L_T$  is the payload height.

After the impact, submunitions debris was recovered and counted. The damage of submunitions can be classified into three levels, namely dented (no liquid leakage), perforated (part of the liquid missing) and smashed (all liquid missing). The damage level definitions and descriptions are as listed in Table 2. The number of submunitions with different damage level are as listed in Table 3. The submunition damage ratio  $P_k = N_k/N$ ,  $N_k$  is the number of damaged submunition (smashed),  $N$  is the total number of the submunitions carried by the payload.

Typical damaged submunitions are as shown in Fig. 4. When  $\xi = 0$ , no submunition survived. Most of the submunitions were seriously damaged, due to the direct hit or the crater generated by the projectile. Some submunitions in the bottom layer (yellow submunitions) were only lightly damaged, mainly due to the impulse loading from one submunition to another, as illustrated in Fig. 4(a).

Typical damage modes of submunition are as shown in Fig. 5. The damage modes of submunition can be dented,

**Table 2. Damage-level definitions of the submunition**

Damage level	Damage type	Damage description
1	Dented	Submunition keeps intact, dented (but no fracture), no fluid missing
2	Perforated	Two cover plates of submunition have no fracture, perforated on the side, part of the fluid missing
3	Smashed	Submunition fractured at one cover plate at least, severe ruptured on the side, all fluids missing

**Table 3. Experimental results of different impact positions**

Test No.	$\xi$	Number of damaged submunition		
		Level 1	Level 2	Level 3
1#	0	0	7	31
2#	-0.17	0	16	22
3#	-0.34	7	17	14
4#	0.17	0	6	32
5#	0.34	2	11	25

perforated, end cover rupture, axial fracture and smashed. Submunitions located in the main damage zone were seriously fragmented (damage level 3) and formed a large number of small irregular debris. The debris distributed far and wide, the weight ranged from 2 g to 100 g and the majority of the debris were more than 6 g. Submunitions which located outside the main damage zone showed various damage levels (damage level 1 and level 2), mainly due to the collision of submunitions with each other, the impact of high-speed fluid, secondary debris and other factors.

The axial fracture mode occurred at the lateral skin of a submunition. When the debris impacted the submunition can, the noticeable inward deformation may induce axial fracture. Also due to the radial high-speed collision of the submunitions with each other, the liquid inside the submunitions generated high pressure and caused the axial fracture. Once the collision occurred at the top portion of the submunitions between each other, it could eventually lead to the joints failure and the cover rupture occurred.



**Figure 4. Typical damaged submunitions (test 1#): (a) Damage level two. (b), (c), (d) and (e) Damage level three.**

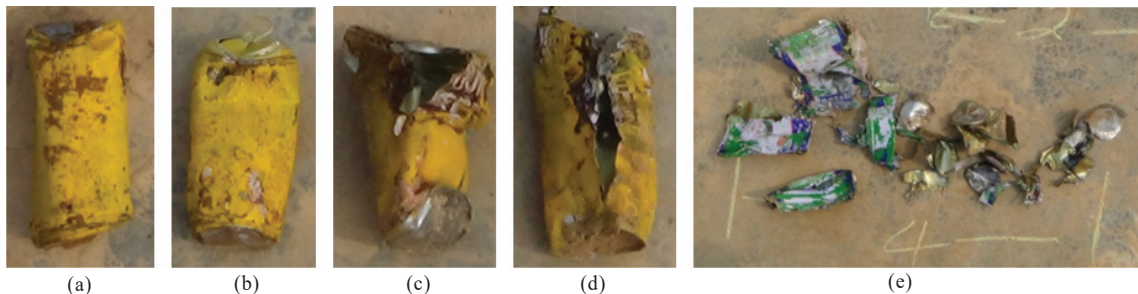


**Figure 5. Typical damage modes of submunition: (a) Dented, (b) Perforated, (c) End covers rupture, (d) Axial fracture, and (e) Smashed.**

### 3. ANALYTICAL MODEL

The collision between projectile and submunition payload is extremely complex. Hence, the models of projectile and submunition payload are simplified. The projectile is simplified as a homogeneous cylindrical structure without regard to the internal structure. The submunition payload is simplified as a semi-infinite target when the crater size is calculated. So submunitions inside the damage zone (the area overlapped by crater volume called damage zone) will be destroyed. Otherwise, submunitions will survive, as shown in Fig. 6.  $v_t$  is the target velocity,  $v$  is the penetrator velocity,  $v_r$  is the relative velocity,  $\alpha$  is the yaw angle,  $\theta_{SA}$  is the strike angle,  $o$  is the aiming point,  $x_a$  is the axial offset,  $y_a$  is the radial offset,  $R_c$  is the crater radius.

Here, Luttwak's oblique theoretical model for penetration<sup>28</sup> which considers the yaw angle is introduced. It is assumed that all the energy is transformed into plastic deformation to form the crater. The penetration depth  $P(\alpha)$  is as given by:

$$P(\alpha) = \frac{\gamma k P(0)(1 + \sin(2\alpha_1))}{\left(\frac{L}{D}\right) \frac{\sin(|\alpha_1|) \cos(\theta)}{\cos(\theta + \alpha_1)} + \gamma k \exp\left(-\frac{|\alpha_1|}{\alpha_c}\right)} \quad (1)$$

where,  $L$  is projectile length,  $D$  is projectile diameter.  $\gamma$  is a constant parameter related to projectile and target material,  $\gamma = 2/3$  [28] is a reasonable value by fitting the data of Yaziv<sup>20</sup>.  $\alpha$  is the yaw angle; parameter  $k$  is related to projectile penetration velocity  $v$ , target yield strength  $Y_T$ , projectile material density  $\rho_p$  and target material density  $\rho_T$ .

$$k = \frac{D_h}{D} \cong \frac{v}{\left(1 + \sqrt{\frac{\rho_T}{\rho_p}}\right) \sqrt{\frac{2Y_T}{\rho_T}}} \quad (2)$$

$D_h$  is the crater diameter.  $P(0)$  is the penetration depth formed by a rod penetrating without yaw, given by the well-known hydrodynamic theory, as

$$P(0) = L \sqrt{\frac{\rho_p}{\rho_T}} \quad (3)$$

Considering the secondary penetration at the rod tail, we will get:

$$P(0) = L \sqrt{\frac{\rho_p}{\rho_T}} + D_h \quad (4)$$

The penetration depth will decrease when projectile penetrates target with yaw angle. For small yaw angle, the rod

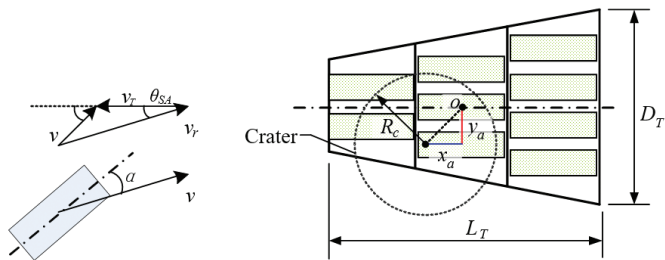


Figure 6. Submunition payload damage determination and definition of associated angles.

will penetrate through the crater without interaction with the wall. The effects of yaw angle become more obvious at angles larger than  $\alpha_c$ , the critical angle:

$$\alpha_c = \arcsin\left(k \frac{D}{L}\right) \quad (5)$$

For large diameter of the resulting hole ( $D_h > L$ ) a critical angle is never reached which means that the rod with its yaw pass through the hole without a strong interaction. Also, when  $\alpha \ll \alpha_c$  the second term in the denominator of Eqn. 1 vanishes.

The unit vector  $\vec{i} = (\vec{n} \times \vec{k}) / |\vec{n} \times \vec{k}|$ ,  $\vec{k}$  is projectile axial direction vector and  $\vec{n}$  is the target plane normal vector, as shown in Fig. 7(a).  $\cos \theta = |\vec{v} \cdot \vec{n}|$ ,  $v_i$  is the velocity component along  $\vec{i}$  direction, while  $\vec{v}_p = \vec{v} - \vec{v}_i$ .  $\alpha_1$  is the angle between velocity component  $\vec{v}_p$  and  $\vec{k}$ , thus  $|\alpha_1| = |\arccos \langle \vec{v}_p, \vec{k} \rangle|$ . For detailed discussion of these formulas see Ref [28]. The width of crater is  $D_h = kD$  and the length of crater is  $L \sin(\alpha)$  when  $\alpha \gg \alpha_c$ , as shown in Fig. 7(b).

The number of damaged submunitions can be predicted with the above damage analytical model. Initial data for projectile  $L=75$  mm,  $D=40$  mm,  $\rho_p=2.76$  g/cm<sup>3</sup>,  $v_r=2468$  m/s and  $Y_p=40$  MPa, for submunition payload  $L_T=417$  mm,  $D_T=313$  mm,  $\rho_T=1.115$  g/cm<sup>3</sup> and  $Y_T=151$  MPa.

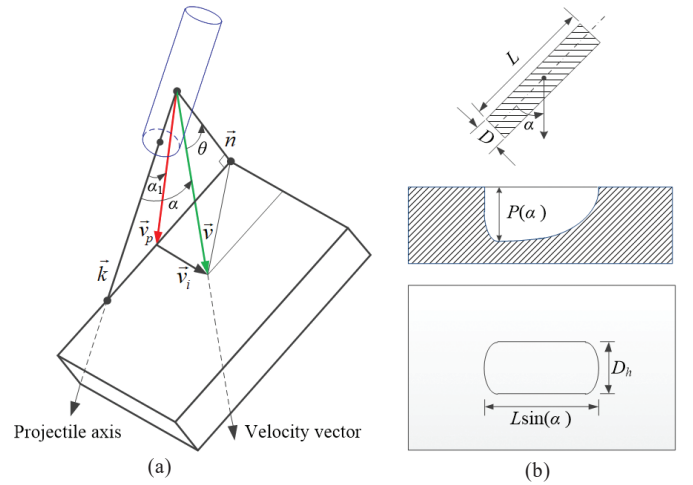


Figure 7. Penetration triangle defining velocity vectors and crater size: (a) Velocity vectors and associated angles and (b) Crater size.

The comparison of total damaged submunition number between experimental data and theoretical prediction data is as shown in Fig. 8. Since the analytical model just accounts for the crater expansion only, experimental data is the number of smashed (damage level three) submunitions which are damaged by direct hit of the projectile. Theoretical prediction results agree well with experimental ones. The maximum and minimum relative error are 22 per cent and 3 per cent, respectively. Even though theoretical analysis model in this paper does not take into account the influence of the collision between submunitions, the secondary debris and other factors, it contains fewer parameters and has high solution efficiency.

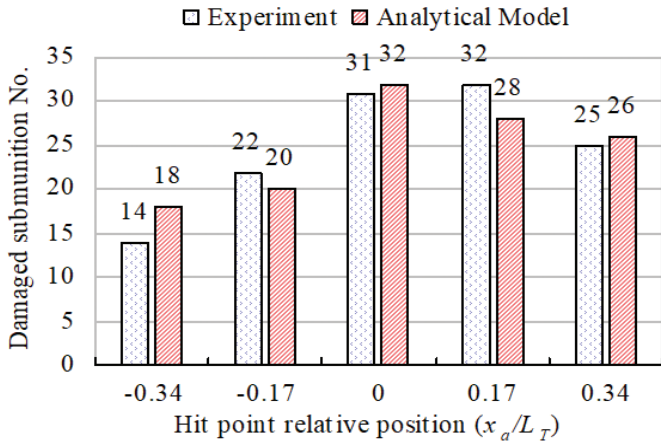


Figure 8. Damaged submunition number comparison between calculations and experiments.

## 4. DISCUSSIONS

### 4.1 Influences of Strike Angle

Here the geometric center of the submunition is chosen as hit-point and the relative impact velocity keeps constant  $v_r=2468$  m/s, while the impact angle and yaw angle change.

Submunition damage ratio of different yaw angle and strike angle are as shown in Fig. 9. It is significantly influenced by both the yaw angle and strike angle. The trend of submunition damage ratio appears to be complex with the increase of strike angle while yaw angle  $\alpha=0^\circ$ , since the number of submunition on the flight path of the projectile changes with the change of strike angle and it is closely related to the submunitions arrangement. When the strike angle  $\theta_{SA}$  is about  $18^\circ$  and yaw angle  $\alpha$  is about  $10^\circ$ , the submunition damage ratio reaches a maximum, hence an appropriate flying attitude of the projectile can create a larger crater volume. This shows that the strike angle has an optimal range for specific submunition payload.

While the strike angle  $\theta_{SA}=90^\circ$ , the projection area of the projectile relative to the payload is calculated by  $A=(\pi D^2/4)\cos(\alpha)+LD\sin(\alpha)$ . When  $\alpha$  is about  $67^\circ$   $A$  reaches maximum. When yaw angle  $\alpha=0^\circ$ , the projection area of projectile along the relative velocity on submunition payload is minimal, the contact area with the payload also is minimal, as well as the crater diameter. The projection area of the projectile will

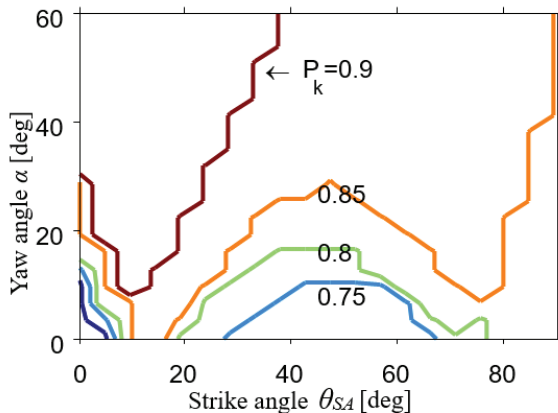


Figure 9. Contours of submunition damage ratio for  $v_r=2468$  m/s,  $x_a=0$ ,  $y_a=0$ ,  $L=75$  mm and  $D=40$  mm.

become larger when the yaw angle increases. This shows that under a specific strike angle with increasing yaw angle, the submunition damage ratio will be increased significantly.

### 4.2 Influences of Hit-point Offset Distance

Here the strike angle  $\theta_{SA}=90^\circ$ , relative impact velocity  $v_r=2468$  m/s, aim point is the geometric center of the submunition payload. The influences of hit-point offset with different yaw angle on submunition damage are analysed. Submunition damage ratio for axial and radial offset are as shown in Figs. 10(a) and 10(b), respectively. With increasing hit-point offset distance ( $x_a < 0$ , offset to the left;  $x_a > 0$ , offset to the right;  $y_a < 0$ , offset to the down;  $y_a > 0$ , offset to the up; see Fig. 6), submunition damage ratio decrease significantly.

Submunition damage ratio is more affected by axial offset distance. The number of submunitions which are overlapped by crater changes a great deal with the hit-point offset distance along the axis direction. Fig. 10(b) shows that submunition damage ratio remain above 0.7 when the radial offset ratio of hit-point  $y_a/D_T$  is within  $\pm 0.2$  range. With the increase of the hit-point offset distance, the submunition damage ratio decreases significantly. Furthermore, yaw angle has less influence on the damage ratio of submunition while  $\theta_{SA}=90^\circ$ , thus the guidance precision is a dominant factor in achieving high submunition damage.

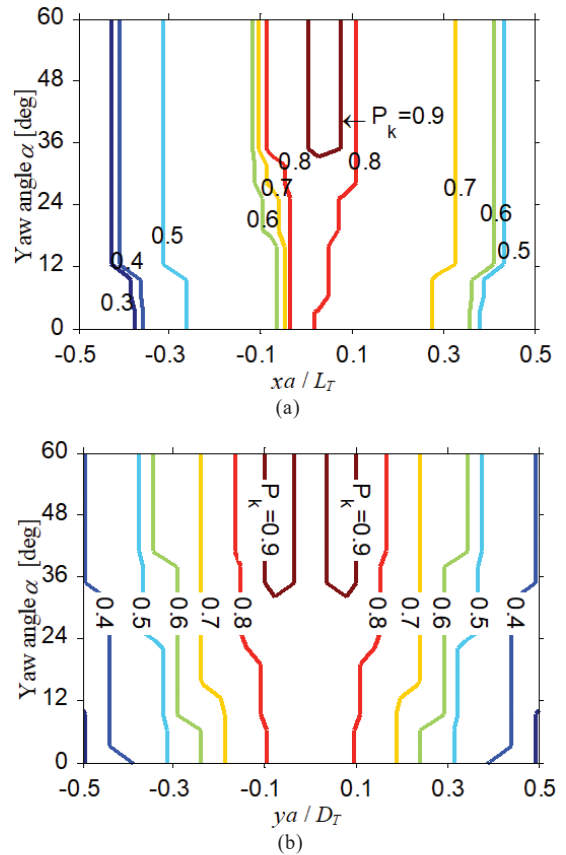
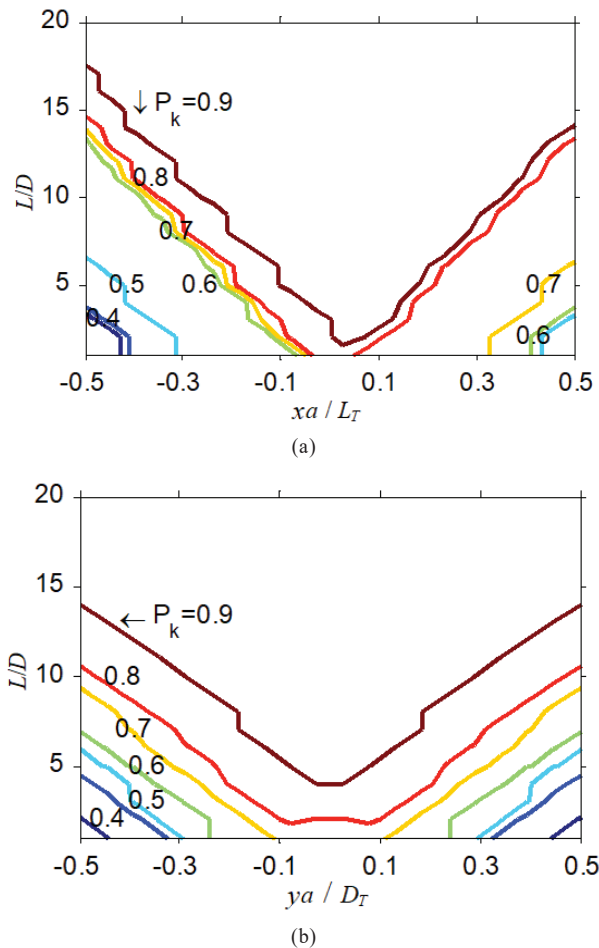


Figure 10. Contours of submunition damage ratio for relative velocity  $v_r=2468$ m/s, strike angle  $\theta_{SA}=90^\circ$ ,  $L=75$ mm and  $D=40$ mm: (a) Hit point away from the geometric center along the symmetry axis and (b) Hit point away from the geometric center along the radial direction.

### 4.3 Influence of Projectile Length to Diameter Ratio

The influence of the projectile length to diameter ratio on submunition payload damage with different hit-point offset distances was analysed. The projectile is 40mm diameter cylinder with a length to diameter ratio ranging from 1 to 20. The strike angle  $\theta_{SA} = 90^\circ$  and the yaw angle  $\alpha = 45^\circ$ . The relative impact velocity  $v_r = 2468$  m/s.

Submunition damage ratio for hit-point axial offset and radial offset with different length to diameter ratio are shown in Figs. 11(a) and 11(b), respectively. The length to diameter ratio and the hit-point position influence the damage ratio of submunition significantly, especially the hit-point offset distance. Under a constant diameter, with the increase of projectile length to diameter ratio, its length increases and the overlap volume become larger, the submunition damage ratio increases. This shows that an appropriate length to diameter ratio can compensate for the large hit-point offset distance. With insufficient guidance precision, increasing the length to diameter ratio of projectile as much as possible can improve submunition damage ratio.



**Figure 11. Contours of submunition damage ratio for relative velocity  $v_r = 2468$  m/s, strike angle  $\theta_{SA} = 90^\circ$ , yaw angle  $\alpha = 45^\circ$ ,  $D = 40$  mm: (a) Hit point away from the geometric center along the symmetry axis and (b) Hit point away from the geometric center along the radial direction.**

### 5. CONCLUSIONS

- (i) The explosively formed projectile technology is effective in investigating the damage effects of the fluid-filled submunitions by high velocity projectile impact.
- (ii) A analytical model for damage which takes into account the yaw angle of a projectile against submunition payload was presented. According to the model, with an appropriate yaw angle of the projectile, the submunition damage ratio could be improved significantly. The smaller the strike angle, the more obvious improvement of submunition damage ratio by increasing the yaw angle.
- (iii) The submunition damage ratio strongly depends upon the hit-point offset distance, showing a significant decrease with increasing hit-point offset distance. It is most sensitive to the axial hit-point offset distance.
- (iv) Length to diameter ratio also influences the submunition damage ratio. The submunition damage ratio can be increased by increasing the length to diameter ratio of the projectile to an appropriate extent. For large hit-point offset distance, increasing the length to diameter ratio of the projectile will effectively improve the submunition damage ratio.

### REFERENCES

1. Lloyd, R.M. Physics of direct hit and near miss warhead technology. American Institute of Aeronautics and Astronautics, 2001, pp. 31. ISBN 1-56347-473-5.
2. Espino, L. Computer modeling for damage assessment of KE-Rod warhead against ballistic missile. Graduate school of the University of Texas at El-Paso, July, 2004.
3. Lloyd, R.M. Near miss warhead technology with multiple effects against submunition payloads. In 9<sup>th</sup> Annual AIAA/BMDO Technology Conference, Osaka, July, 2000.
4. Louie, N. & Hambleton, J. Multi-dimensional analysis of TMD lethality data. Boeing North American Canoga Park CA Rocketdyne Div., Los Angeles, USA, 1998.
5. Willis, J. Missile defense: Sorting out collateral damage. Army Space Journal, Spring/Summer Edition, 2011, pp. 44-49.
6. Hildreth, S.A. Kinetic energy kill for ballistic missile defense: A status overview. Congressional Research Service Reports, 2007.
7. Liu, J.; Long, Y.; Ji, C.; Liu, Q.; Zhong, M. & Ge, S. Ballistic performance study on the composite structures of multi-layered targets subjected to high velocity impact by copper EFP. *Compos. Struct.*, 2017, **184**, 484-496. doi:10.1016/j.compstruct.2017.09.072.
8. Forrestal, M.J. & Piekutowski, A.J. Penetration experiments with 6061-T6511 aluminum targets and spherical-nose steel projectiles at striking velocities between 0.5 and 3.0 km/s. *Int. J. Impact Eng.*, 2000, **24**(1), 57-67. doi: 10.1016/S0734-743X(99)00033-0.
9. Arnold, W. & Rottenkolber, E. Lethality enhancer against TBMs with demanding submunition payloads, In 24<sup>th</sup> International symposium on ballistics. New Orleans, Louisiana, USA: 2008, pp. 1027-1034.
10. Carver, D.; Campbell, L. & Roebuck, B. Large-scale, hypervelocity, high-fidelity interceptor lethality

- development in AEDC's range G. *Int. J. Impact Eng.*, 2008, **35**(12), 1459-1464.  
doi: 10.1016/j.ijimpeng.2008.07.036.
11. Melchor-Lucero, O. & Carrasco, C. J. Computational technique to assess warhead lethality against ballistic missile. *J. Aerospace Eng.*, 2009, **22**(4), 354-364.
  12. Chang, Y. Hydrocode analysis at APL, Johns Hopkins APL technical digest, 1998, **19**(1), 73.
  13. Baudin Gallic, C. & Rouquand, A. Lethality criteria to defeat ballistic missile HE and chemical payloads. French Ministry of Defense, France, 2004.
  14. Børvik, T.; Langseth, M.; Hopperstad, O.S. & Malo, K.A. Perforation of 12 mm thick steel plates by 20-mm diameter projectiles with flat, hemispherical and conical noses: Part I: experimental study. *Int. J. Impact Eng.*, 2002, **27**(1), 19-35.  
doi: 10.1016/S0734-743X(01)00034-3.
  15. McHenry, M. R.; Levin, M. A. & Orphal, D. L. Estimating optimum hit-to-kill vehicle configurations for lethality against submunition payloads. *Inb36<sup>th</sup> Aiaa Aerospace Sciences Meeting and Exhibit*, Reno, NV, USA, Jan 1998.  
doi:10.2514/6.1998-831.
  16. Doup, P. W. Endgame analyses against a ballistic missile a parametric study, TNO Defense, Security and Safety, 2005.
  17. Jin, X.; Yu, Q.; Wang, Y.; Gong, J.; Zheng, Y. & Wang, H. Lethality analytical model of hit-to-kill kinetic kill vehicle against submunition payloads. *T. B. Inst. Techno.*, 2015, **35**(10), 1016-1021.  
doi: 10.15918/j.tbit1001-0645.2015.10.006.
  18. Karpp, R. Lethality estimates of two different kill vehicles based on SPHINX hydrocode simulation. Raytheon Electronic Company, 1996.
  19. Warren, T.L. & Poormon, K.L. Penetration of 6061-T6511 aluminum targets by ogive-nosed VAR 4340 steel projectiles at oblique angles: Experiments and simulations. *Int. J. Impact Eng.*, 2001, **25**(10), 993-1022.  
doi: 10.1016/S0734-743X(01)00024-0.
  20. Yaziv, D.; Walker, J.D. & Riegel, J.P. Analytical model of yawed penetration in the 0 to 90 degrees eange. *In Proceedings of the 13<sup>th</sup> International Symposium on Ballistics*, Stockholm, Sweden, 1992, **3**, 17-23.
  21. Behner, T.; Hohler, V.; Anderson Jr, C.E. & Goodlin, D. Influence of yaw angle on the penetration reduction of long rods in oblique targets. *In 20<sup>th</sup> International Symposium on Ballistics*, Orlando, Florida, 2002, pp. 834.
  22. Schonberg, W.P.; Bean, A.J. & Darzi, K. Hypervelocity impact physics, NASA-CR-4343, January, 1991.
  23. Wilbeck, J. S.; Herwig, S. B.; Kilpatrick, J. M.; Faux, D.R.; Weir, R.J.; Hertel, E.S. & Dutta, M.K. Hypervelocity impact of spaced plates by a mock kill vehicle. *Int. J. Impact Eng.*, 2001, **26**(1), 853-864.  
doi: 10.1016/S0734-743X(01)00139-7.
  24. Nutting, J. Frequently asked questions, www.canmaker.com, 2011.
  25. Cardoso, D. & Teixeira-Dias, F. Modelling the formation of explosively formed projectiles (EFP). *Int. J. Impact Eng.*, 2016, **93**, 116-127  
doi: 10.1016/j.ijimpeng.2016.02.014.
  26. Li, R.; Li, W. & Wang, X. Effects of control parameters of three-point initiation on the formation of an explosively formed projectile with fins. *Shock Waves*, 2017, **28**(5), 1-14.  
doi: 10.1007/s00193-017-0725-9.
  27. Hu, F.; Wu, H.; Fang, Q.; Liu, J.; Liang, B. & Kong, X. Impact performance of explosively formed projectile (EFP) into concrete targets. *Int. J. Impact Eng.*, 2017, **109**, 150-166.  
doi: 10.1016/j.ijimpeng.2017.06.010.
  28. Luttwak, G. Oblique and yawed rod penetration. *In 5<sup>th</sup> International Symposium on Behaviour of Dense Media under High Dynamic Pressures, HDP5*, France, 23-27 Jun, 2003.

#### ACKNOWLEDGEMENT

The support of National High Technology Research and Development Program (863 Program) (No. AA8016028C) is gratefully acknowledged.

#### CONTRIBUTORS

**Mr Zan Yang** obtained his MSc (Computer Science and Technology) from Beijing Institute of Technology, in 2007. Currently he is pursuing PhD (Armament Science and Technology) from Beijing Institute of Technology. His research activity and interest are focused on new concept ammunition and high efficiency damage technology, target vulnerability analysis and simulation technology.

The contribution in this study is related to making idea and concept of study, collating and analysing experimental data, and writing the article.

**Dr Zheng Yuan-feng** obtained his PhD (Armament Science and Technology) from Beijing Institute of Technology, in 2012. Currently, he is a Lecturer of State Key Laboratory of Explosion Science and Technology, Beijing Institute of Technology. His main research direction is new concept ammunition and high efficiency damage technology.

The contribution in this study is related to conducting experiment.

**Dr Yu Qing-bo** obtained his PhD (Armament Science and Technology) from Beijing Institute of Technology, in 2010. Currently, he is an Associate Professor of State Key Laboratory of Explosion Science and Technology, Beijing Institute of Technology. His research activity and interest are focused on new concept ammunition and high efficiency damage technology, target vulnerability analysis and simulation technology.

The contribution in this study is related to designing the EFP device.

**Prof. Wang Hai-fu** obtained his PhD (Ammunition Warhead Engineering) from Beijing Institute of Technology, in 1996. Currently, he is a Professor and Doctoral Tutor in State Key Laboratory of Explosion Science and Technology, Beijing Institute of Technology. His research activity and interest are focused on new concept ammunition and high efficiency damage technology, target vulnerability analysis and simulation technology, space-based weapons and space attack and defense technology, space debris and spacecraft protection technology.

The contribution in this study is related to making idea and concept of study, defining of the model of the experiment and participation in the creation and review of article